Preferential gene expression in the limbus of the vervet monkey

Zhenhua Ding,[1] Jun Dong,[2] Jason Liu,[2] Sophie X. Deng[1]

[1]Cornea and Uveitis Division, Jules Stein Eye Institute, University of California, Los Angeles, CA; [2]Department of Human Genetics, University of California, Los Angeles, CA

Purpose: To elucidate the unique molecular factors and biological processes that are differentially expressed in the limbal stem cell microenvironment by comparing directly to that of its immediate adjacent structures, the cornea and conjunctiva.
Methods: Total RNA was isolated and amplified from the limbus, cornea, and conjunctiva. A gene expression profile of each tissue type was obtained by using microarray technique. The transcripts in which the expression level was at least twofold higher than that in the other two tissue types were identified. The expression levels of selected genes were confirmed by quantitative reverse transcription polymerase chain reaction (QRT–PCR). Protein expression of selected genes were confirmed by an immunohistochemistry study in normal human ocular tissue.
Results: There were 186 preferentially overexpressed transcripts in the limbus in direct comparison to that in the cornea and conjunctiva. Many signature genes in the cornea and conjunctiva were among the preferentially expressed transcripts obtained by the microarray data. In addition, a significant number of new genes were identified, and the expression level of all nine selected genes was verified by QRT–PCR. Protein expression levels of keratin 13, tenascin c, homeodomain only protein (HOP), and TP53 apoptosis effector (PERP) were confirmed in human ocular tissues. Functional analysis of the preferentially expressed genes in the limbus reviewed that melanin metabolism and cell-cell adhesion were among the noticeable biological processes. Chromosomal distribution of the overexpressed genes in the limbus was disproportional to that of all known human genes.
Conclusions: These findings may shed light on the unique molecular components and regulation of limbal stem cells and their niche.

Corneal epithelial stem cells have been suggested by clinical and experimental evidence to reside at the basal layer of the limbal epithelium, and they are so called "limbal stem cells" (LSCs) [1-5]. Many molecules have been proposed as markers of LSCs [6-8]. However, there is no unique marker to directly identify LSCs, and this significantly limits the localization and characterization of LSCs and their niche [9].

The concept of stem cell niche was first introduced by Schofield in 1978 [10]. The stem cell fate is governed by intrinsic and extrinsic signals. The surrounding microenvironment or niche, which consists of niche cells, soluble factors, and extracellular matrix, provides the external signals. The underlying limbal stroma including the extracellular matrix, vascular supply, and stromal cells appears to modulate the differentiation and survival of corneal epithelial cells [9,11-13]. Because LSCs have not yet been located directly, the exact spatial arrangement of LSCs and their niche cells is largely unknown. Goldberg and Bron [14] suggested that LSCs are located within the specific limbal structure, the palisades of Vogt. Papillary projections of the stroma extend upward at the basement of the limbus, and distinct invaginations of limbal epithelium into the deep stroma (limbal crypt) appear similar to the epithelial crypts of

the gut where the intestinal epithelial stem cells are located [1,15,16]. The LSC niche has been proposed to reside within these deep limbal crypts [17,18].

To understand the intrinsic factors that characterize limbal stem cells, the gene expression profile of limbal epithelial cells has been compared with that of corneal epithelial cells [19,20] or of conjunctival epithelial cells [21], but no study comparing the gene expression profiles of all three types of epithelia with the underlying stroma has been reported. The goal of the present study was to identify unique genes and biological pathways that are differentially expressed in the limbal epithelium and the underlying stroma in comparison with those in the cornea and conjunctiva. The underlying stroma was included to ensure that the samples contained the deep limbal crypts and the potential components of LSC niche.

METHODS

Tissue collection: Eye tissue of vervet monkeys (Chlorocebus aethiops sabaeus) was obtained from the Department of Human Genetics at the University of California, Los Angeles, CA, through the tissue-sharing protocol adherence to the ARVO Statement for the Use of Animals in Ophthalmic and Vision Research and was approved by the Institutional Animal Research Committee of the University of California, Los Angeles. The age of the animal varied from 32 to 37 months, and the diameters of the corneas were between 10 and 11 mm. The intact globe was enucleated within 1 h after

---

Correspondence to: Sophie X. Deng, M.D., Ph.D., Cornea and Uveitis Division, Jules Stein Eye Institute-UCLA, 100 Stein Plaza, Los Angeles, CA, 90095; Phone: (310) 794-7371; FAX: (310) 794-7906; email: deng@jsei.ucla.edu

euthanasia, flash-frozen on dry ice, and stored at −80 °C. The globe was placed at −5 °C to soften the tissue to allow tissue dissection. The cornea was trephined with an 8.0 mm trephine, and the epithelium along with the stroma immediately beneath it (one-third to one-half of the total stroma) was dissected. The conjunctiva with the underlying Tenon and the 1.5 to 2 mm rim of the limbal epithelium with the stroma immediately beneath it (one-third to one-half of the total stroma) were also dissected. All dissected tissues were stored at −80 °C until the RNA was extracted.

RNA isolation: To ensure complete homogenization, a serrated homogenizer (Omni International, Marietta, GA) was used. All samples were kept on dry ice before homogenization. Each sample was bathed in a lysis buffer provided in Qiagen RNeasy mini kits (Qiagen, Valencia, CA). β-Mercaptoethanol (Invitrogen, Carlsbad, CA) was added to the lysis buffer in a 1:100 ratio. In between periods of homogenization, the blade was rinsed twice with filtered distilled deionized (ddI) water (Millipore, Billerica, MA), once with 70% ethanol, and twice in fresh Millipore ddI water. Total RNA was isolated by using the Qiagen RNeasy mini columns (Qiagen). The quantity and quality of the extracted total RNA were assessed by the NanoDrop 1000 spectrophotometer (NanoDrop, Wilmington, DE) and the 2100 Bioanalyzer (Agilent Technologies, Santa Clara, CA). Because of the sample's low concentration, all integrity checks were run on Agilent's RNA Pico Chips.

Microarray analysis: A standard starting amount of total RNA (10 ng) was used for two-round transcription amplification. Synthesis for all samples was successful and provided a sufficient yield of cRNA. Vervet monkey arrays were not available, and human arrays had previously been used for other primate gene profiling without discernible loss of information. Use of human arrays for other primate gene expression studies has been very productive [22,23]. Affymetrix U133 plus 2.0 human expression arrays (Affymetrix, Santa Clara, CA) was used in accordance with the standard Affymetrix protocol for eukaryotic expression arrays. All microarrays were scanned by using an Affymetrix 3000 one-color microarray scanner. Raw images were examined for surface defects and for proper grid placement. Background intensity, housekeeping gene expression, and a 3′- to -5′ ratio of probe sets for genes of varying lengths were also used to assess the quality. Probe intensity values were generated by using the Affymetrix Gene Chip Operating System.

Quantitative real-time polymerase chain reaction: Total unamplified RNA was used for reverse transcription. Gene-specific primers were designed (Table 1). The cDNA of each transcript was reverse-transcribed by using Superscript II RNase H2 reverse transcriptase (Invitrogen) according to the manufacturer's recommendations, in triplicate. The relative abundance of transcripts was detected using a Stratagene Mx3000P real-time polymerase chain reaction (PCR) system with Brilliant SYBR Green QRT–PCR Master Mix (Stratagene, La Jolla, CA). Cycling conditions were as follows: an initial denaturing step of 5 min at 94 °C and subsequent 40 cycles of amplification in which each cycle consisted of 15 s at 94 °C, 30 s at 55 °C, and 30 s at 72 °C. To generate a dissociation curve after the amplification cycles, each sample was incubated at 95 °C for 1 min followed by a melting curve program (55-99 °C with a 5 s hold at each temperature). The fluorescence intensity of each sample was acquired during the execution of the melting curve program and normalized in relation to that of the housekeeping gene, glyceraldehyde-3-phosphate dehydrogenase (GAPDH). The average value of the triplicates from each transcript was used for comparison.

Data analysis: All Affymetrix data were normalized by using the justRMA algorithm of R software from the Bioconductor group [24], which implements the RMA (robust multi-array average) normalization method [25]. In this normalization step, each array was individually normalized by combining it with a pool of 50 fixed reference arrays in the Microarray Core Facility at the University of California, Los Angeles. Genes with expression values at least twofold greater than those in the other two tissue types were selected and considered to be differentially expressed. EASE (expression analysis systematic explorer) software (NIH, Frederick, MD) was used for functional analysis [26]. Lists of differentially expressed genes were checked by EASE to find the most over-represented gene groups.

Immunohistochemistry: Human sclerocorneal tissues were obtained from the San Diego Eye Bank (San Diego, CA). The death to preservation time was less than 12 h. The tissue was then cut into four quadrants and embedded in OCT on dry ice within six days from procurement. Tissues were cut into to 6 μm sections using cryostat and stored in −80 °C. Rabbit polyclonal anti-tenascin c (TNC) and anti-keratin13 (K13) antibodies were obtained from Santa Cruz Biotechnology Inc. (Santa Cruz, CA). The polyclonal rabbit anti-HOP [27] was a generous gift from Dr. Eric Olson (University of Texas Southwestern Medical Center at Dallas, Dallas, TX), and the rabbit anti-PERP antibody was from Abcam (Cambridge, MA). Frozen section slides were warmed up in the desiccator at room temperature, fixed with 4% formaldehyde for 20 min, washed with 0.3% triton in phosphate buffer saline (PBS) three times, and blocked with 5% normal goat serum (Jackson ImmunoResearch Laboratories, West Grove, PA) in PBS for 30 min. The slides were washed with 1% BSA/PBS three times, and incubated with primary antibodies overnight at 4 °C. The slides were washed with 1% BSA/PBS three times and labeled with the appropriate secondary antibodies, Alexa Fluor 488 goat anti rabbit IgG or Alexa Fluor 488 goat anti mouse IgG (Invitrogen) for 1 h at room temperature. The nucleus was labeled with Hoechst 33342 at 0.5 μg/ml for 10

TABLE 1. PRIMERS USED FOR QRT–PCR.

Gene name	Direction	Primer sequence
MYBPC1	Forward	TCCAGATTGTTGACCGTCCA
	Reverse	CACTGAGGCCGCACATGTT
TYRP1	Forward	GGTGCAACGTCTTCCTGAACC
	Reverse	CATCAAAGACTGCATCCGTGA
K13	Forward	CAGAGCGTGGAGGCTGACAT
	Reverse	CCTCCTTGTTCAGCTCTGCAC
WIF1	Forward	CACCTGCTTTAACGGAGGGAC
	Reverse	CAGTGTCTTCCATGCCAACCT
HPGD	Forward	GGTGAAGGCGGCATCATT
	Reverse	GCAATCAATGGTGGGTCCA
HOP	Forward	ATGTCGGCGGAGACCGCGAGCGG
	Reverse	TTAGTCTGTGACGGATCTGCAC
TNC	Forward	GTGGAGAGCTTCCGGATTACC
	Reverse	TACTCCACTGTGTTCCCGGAC
PERP	Forward	CTGCTCCTACTCAGCGCCAT
	Reverse	CAAAGCCGTAGGCCCAGTTAT
K12	Forward	CCAGGTGAGGTCAGCGTAGAA
	Reverse	CCTCCAGGTTGCTGATGAGC
GAPDH	Forward	CGACCACTTTGTCAAGCTCA
	Reverse	AGGGGTCTACATGGCAACTG

Abbreviations: MYBPC1, myosin binding protein C; TYRP1, tyrosinase-related protein 1; K13, keratin 13; WIF1, Wnt inhibitory factor 1; HPGD, hydroxyprostaglandin dehydrogenase 15-(NAD); HOP, homeodomain-only protein; TNC, tenascin C; PERP, TP53 apoptosis effector; K12, keratin 12; GAPDH, glyceraldehyde-3-phosphate dehydrogenase.

min. The slides were washed with PBS three times and mounted. The pictures were taken under 25X object using a Zeiss fluorescent microscope (Carl Zeiss Inc., Oberkochen, Germany).

RESULTS

The RNA yield was 568.2 ng, 60 ng, and 371.4 ng from the limbus, cornea, and conjunctiva, respectively. The RNA quality assessed by using the Pico Chip revealed a flat baseline with no significant tailing of the rRNA bands (data not shown), and the S18 to S23 ratio was between 1.8 and 2.0. The RNA isolated from all three tissues appeared to have little degradation.

To investigate the overall gene expression profiles of the limbus, conjunctiva, and cornea, we used the Affymetrix Human U133 plus 2.0 array, which contains 54,675 probe sets representing approximately 47,000 transcripts and variants. The Affymetrix U133 plus 2.0 human expression array was chosen because of the relatedness between humans and other primates. The RMA normalized data from all three tissue types were deposited into the Gene Expression Omnibus (accession number GSE10683). The pairwise scatter plots of the normalized values indicated an overall similarity in gene expression among the three tissue types (Figure 1). A closer correlation was observed between the limbus and cornea (r=0.96) and between the limbus and conjunctiva (r=0.95) while a slightly lesser correlation was seen between the cornea and conjunctiva (r=0.90). The gene in which expression in one tissue was at least twofold higher than that in the other two

tissues was considered to be differentially expressed. There were 186 transcripts predominantly overexpressed in the limbus, 644 in the cornea, and 506 in the conjunctiva. Of the 186 preferentially expressed transcripts in the limbus, 172 encoded proteins with known functions. The preferentially overexpressed genes in the limbus were ranked based on the average ratio of expression against those in the cornea and conjunctiva. The top 50 transcripts were listed in Table 2.

To validate our microarray data, we analyzed the expression pattern of several well known signature genes in the cornea and conjunctiva. One of the cornea epithelium markers, keratin 12 [2], and the cornea stroma protein, keratocan [28], were predominantly expressed in the cornea and minimally expressed in the conjunctiva and limbus (Figure 2). Mucin 5AC, a conjunctiva marker [29], was preferentially expressed in the conjunctiva but not in the other
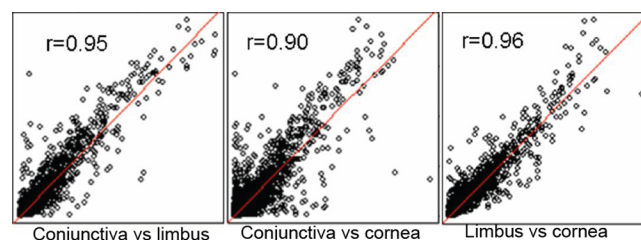

Figure 1. Pairwise scatter plot analysis of the correlation of all transcripts among the limbus, cornea, and conjunctiva indicated an overall similarity among all three tissue types. A slightly lower correlation was seen between the conjunctiva and cornea.

TABLE 2. THE TOP 50 PREFERENTIALLY OVEREXPRESSED TRANSCRIPTS IN THE LIMBUS THAT WERE SELECTED ACCORDING TO THE RANKING OF THE AVERAGE RATIO OF EXPRESSION LEVEL.

Gene title	Gene symbol	Public ID	Average ratio
Cell adhesion			
myosin binding protein C, slow type	MYBPC1	BF593509	23.4
Collagen, type VIII, alpha 1	COL8A1	AL359062	5.04
desmoglein 3 (pemphigus vulgaris antigen)	DSG3	AI813438	4.85
cadherin 6, type 2, K-cadherin (fetal kidney)	CDH6	AU151483	4.06
Protocadherin 9	PCDH9	R49295	3.62
tenascin C (hexabrachion)	TNC	NM_002160	6.55
Developmental process			
keratin 13	KRT13	NM_002274	11.04
tumor necrosis factor receptor superfamily, member 19	TNFRSF19	BF432648	7.72
secretogranin II (chromogranin C)	SCG2	NM_003469	6.02
WNT inhibitory factor 1	WIF1	NM_007191	5.61
v-jun sarcoma virus 17 oncogene homolog (avian)	JUN	NM_002228	3.9
mohawk homeobox	MKX	AW023227	3.67
Neurological and nervous system development			
coagulation factor C homolog, cochlin (Limulus polyphemus)	COCH	BC007230	6.43
retinol binding protein 4, plasma	RBP4	NM_006744	6.15
proenkephalin	PENK	NM_006211	5.39
proteolipid protein 1 (Pelizaeus-Merzbacher disease, spastic paraplegia 2, uncomplicated)	PLP1	BC002665	5.12
paired box gene 3 (Waardenburg syndrome 1)	PAX3	AA194168	4.31
very low density lipoprotein receptor	VLDLR	L22431	8.75
Netrin G1	NTNG1	AW051597	7.22
pleiotrophin (heparin binding growth factor 8, neurite growth-promoting factor 1)	PTN	AL565812	3.44
sodium channel, voltage-gated, type II, beta	SCN2B	AA447729	3.41
Melanin metabolic process			
tyrosinase-related protein 1	TYRP1	NM_000550	19.16
tyrosinase (oculocutaneous albinism IA)	TYR	BC027179	5.58
dopachrome tautomerase (dopachrome delta-isomerase, tyrosine-related protein 2)	DCT	NM_001922	4.27
Transport			
six transmembrane epithelial antigen of the prostate 1	STEAP1	NM_012449	8.08
solute carrier family 7 (cationic amino acid transporter, y+ system), member 2	SLC7A2	AA876372	6.44
solute carrier family 35, member F3	SLC35F3	BF968270	4.88
solute carrier family 16 (monocarboxylic acid transporters), member 6	SLC16A6	AI873273	4.79
potassium voltage-gated channel, shaker-related subfamily, member 2	KCNA2	BF513715	3.54
solute carrier family 28 (sodium-coupled nucleoside transporter), member 3	SLC28A3	NM_022127	3.52
Others			
unknown	unknown	H99792	10.3
phosphoenolpyruvate carboxykinase 1 (soluble)	PCK1	NM_002591	9.6
Transcribed locus, moderately similar to NP_775622.1 transmembrane protein 28	unknown	H09780	8.98
hydroxyprostaglandin dehydrogenase 15-(NAD)	HPGD	NM_000860	6.61
glutathione peroxidase 2 (gastrointestinal)	GPX2	NM_002083	6.6
melan-A	MLANA	U06654	5.94
roundabout, axon guidance receptor, homolog 2 (Drosophila)	ROBO2	AB046788	5.33
CAZ-associated structural protein	CAST1	Z38645	5.23
lipoma HMGIC fusion partner-like 3	LHFPL3	AI939602	5.06
Chromosome 8 open reading frame 42	C8orf42	AI632224	4.97
brain-specific angiogenesis inhibitor 3	BAI3	NM_001704	4.87
adenylate cyclase 1 (brain)	ADCY1	AL120173	4.65
hypothetical protein LOC283713	LOC283713	T03743	4.52
sushi domain containing 4	SUSD4	BC004888	3.77
L-threonine dehydrogenase	TDH	NM_152566	3.76
zinc finger protein 236	ZNF236	AA004757	3.68
family with sequence similarity 107, member B	FAM107B	BC004872	3.55
chromosome 1 open reading frame 74	C1orf74	AW295407	3.53
low density lipoprotein receptor-related protein 11	LRP11	BF696304	3.51
EPS8-like 1	EPS8L1	AF282167	3.51

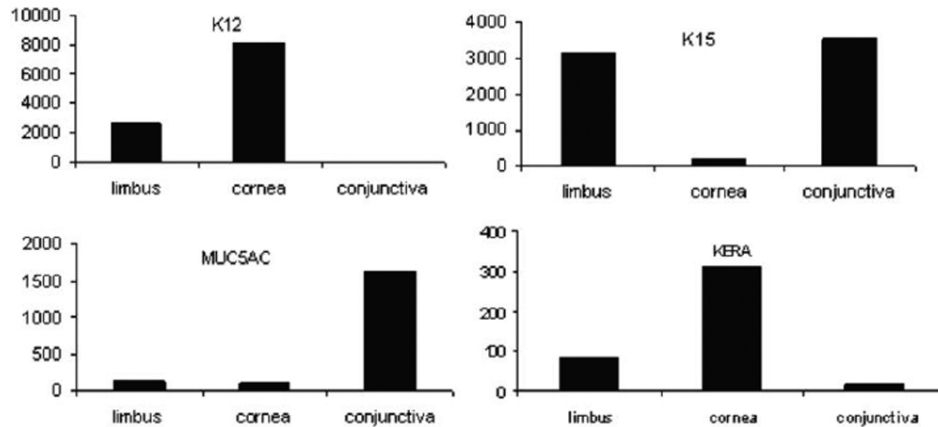The transcripts were grouped based on their function.

Figure 2. Expression levels of selected signature genes in the cornea and conjunctiva obtained by the microarray method. Abbreviations: K12, keratin 12; K15, keratin15; MUC5AC, mucin 5AC; KERA, keratocan.

two tissues (Figure 2). Other markers such as keratin 15, which had been shown to be exclusively expressed at the basal epithelial layer of the limbus and conjunctiva [30], had a higher transcription level in the limbus and conjunctiva (Figure 2). The expression levels of all of these signature genes of each tissue type were highly correlated with their expected expression patterns.

To further verify the microarray method, nine transcripts with differential expression patterns seen in our microarray analysis were independently quantified by QRT-PCR. These genes included Wnt inhibitory factor 1 (WIF1), hydroxyprostaglandin dehydrogenase (HPGD), K13, K12, HOP, PERP, myosin binding protein C (MYBPC1), tyrosinase-related protein 1 (TYRP1), and TNC. To allow for direct comparison of these two methods, the highest expression value of each gene obtained by each method was independently set to 1. The expression values in the other two tissue types were calibrated proportionally for each method. In all cases, the expression levels of all nine genes seen in the microarray experiment were consistent with those measured by QRT–PCR (Figure 3).

Expression of K13, TNC, PERP, and HOP at the protein level was further studied in human ocular tissues by immunohistochemistry. As showed in Figure 4, K13 was expressed at the suprabasal level of limbal and conjunctival epithelium. It was absent at the basal level in both tissues. The level of expression was higher at the limbus and totally absent in the cornea. TNC is a nonstructural extracellular matrix protein that is believed to regulate cell adhesion and migration and to have signal-altering functions [31,32]. It was expressed at the basement membrane of the basal limbal epithelium and blood vessel walls and was absent in the cornea and conjunctiva. HOP was expressed in the nucleus of a subgroup of basal epithelial cells and deep stromal cells in the limbus. It was also found in the basal layer of the conjunctival epithelium and a smaller population of stromal cells but at a much lower level than in the limbus. It was completely absent in the corneal epithelium and stroma.

EASE software was used to identify gene ontologies that were preferentially expressed in the limbus. Many important biological processes were identified. A few noticeable pathways included melanin biosynthesis and metabolism, ectoderm development, neurophysiologic processes, and cell adhesion. Melan-A, a melanocyte differentiation antigen [33], was predominantly expressed in the limbus. Melanin biosynthesis is mediated by a group of enzymes that is uniquely expressed in melanocytes and belongs to the tyrosinase-related protein (TRP) family. TYRP1 is one of the most abundant glycoproteins in melanocytic cells [34].Three members of the TRP family, tyrosinase (TYR), TYRP1, and dopachrome tautomerase (DCT, formally known as tyrosinase-related protein 2) [35-38], were among the top out of the 50 highly expressed genes in the limbus (Table 2).

Seven highly expressed transcripts in the limbus encode proteins that are involved in cell-cell adhesion or are components of the extracellular matrix. These proteins include TNC [39]; P-cadherin [40,41]; K-cadherin [42,43]; collagens type XI α1 [44], type VII α1 [45,46], and type VIII α1 [47]; and desmoglein [48]. All of these proteins have been implicated in the development of the cornea, the regulation of cell adhesion and migration, or the alternation of intracellular signaling.

Genes encoding human proteins were not uniformly distributed on different chromosomes, and previous studies showed that there was tissue-specific organization of genes on human chromosomes [49]. We therefore identified the chromosomal localization of the 172 transcripts of known functions that are preferentially overexpressed in the limbus and compared to the chromosomal localization of all known human genes. The analysis showed that the highest percentage of the limbus-specific genes was found on chromosome 15 when compared with that of all other known human genes (6.98% versus 3.01%). The next highest percentage was found on chromosome 14 (5.23% versus 3.23%), and the lowest percentage was found on chromosome 19 (0.58% versus 4.79%; Figure 5).
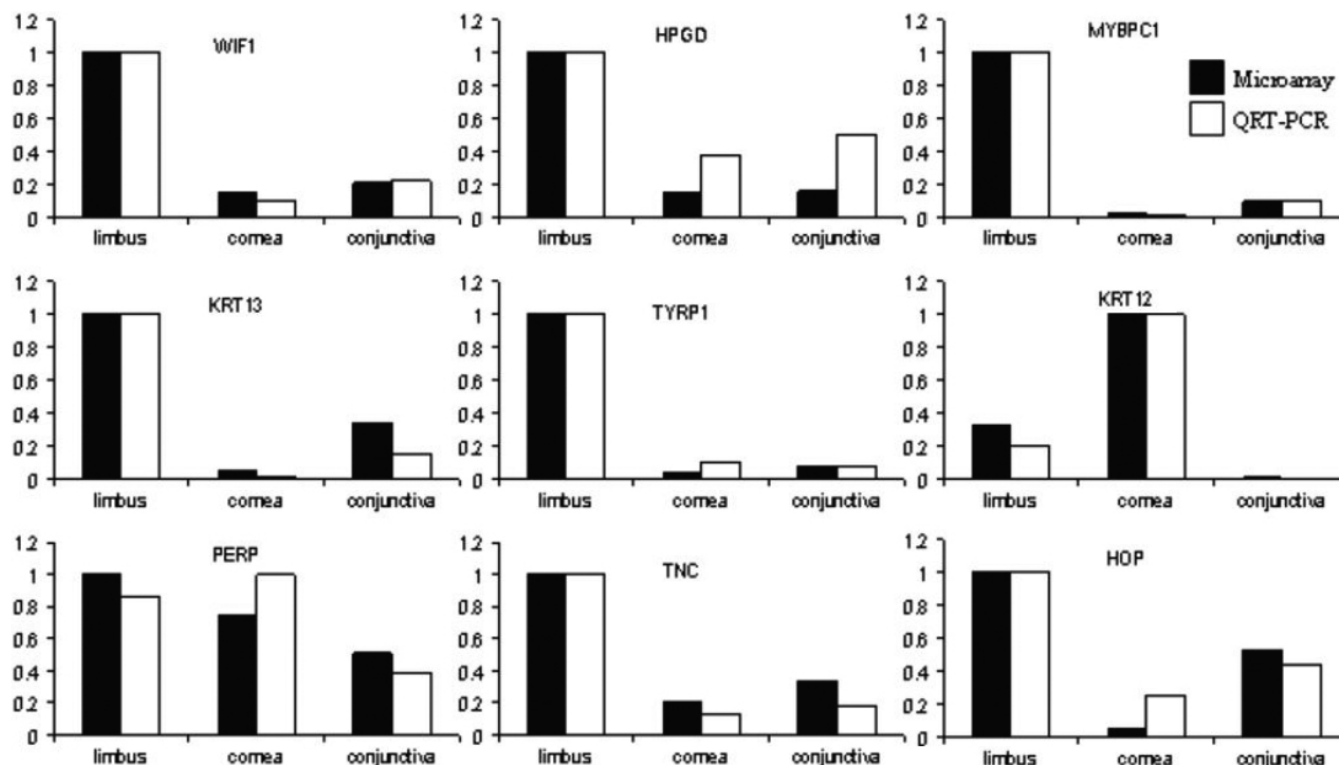
Figure 3. Levels of mRNA of nine transcripts obtained by microarray method were comparable to those obtained by QRT–PCR. Solid bars represent expression values obtained by microarray, and the white bars represent expression values obtained by QRT–PCR. Abbreviations: WIF1, Wnt inhibitory factor 1; HPGD, hydroxyprostaglandin dehydrogenase 15-(NAD); MYBPC1, myosin binding protein C; TYRP1, tyrosinase-related protein 1; KRT12, keratin 12; KRT13, keratin 13; PERP, TP53 apoptosis effector; TNC, tenascin C; HOP, homeodomain-only protein.

DISCUSSION

This study is the first to investigate the gene profile of the limbus in direct comparison with those of two adjacent structures, the cornea and conjunctiva, in the vervet monkey. The purpose of this study is to elucidate potential molecular components of the LSC niche. The epithelia and the underlying stroma are included in the analysis. The advantage of this approach allows for comparing all different cell types simultaneously to identify the unique transcript in all cell types. One limitation of the approach is that the spatial location of the transcript needs to be further verified by immunohistochemistry.

To overcome the difficulty of obtaining sufficient fresh human ocular tissues, we used ocular tissues of the vervet monkey because the monkey genome is more than 95% similar to that of the human. All three tissues types were acquired from the same eye to reduce variations seen among different animals. Many signature genes of the cornea and conjunctiva were among the preferentially expressed genes in our microarray analysis (Figure 2). In addition, the expression levels of nine selected transcripts observed in the microarray experiment were consistent with those seen in our independent QRT–PCR analysis. Protein expression of K13, HOP, PERP, and TNC in all three tissue types in humans

corresponded very well to their mRNA levels detected by both microarray and QRT–PCR methods. These results further validate the microarray data.

ATP-binding cassette member 2 (ABCG2) and ΔNp63α have been proposed as potential LSC markers. Our data showed that ABCG2 was expressed in the conjunctiva at the highest level (124) followed by the limbus (75), which was consistent with the previous finding that conjunctiva contained a higher portion of the side population than the limbus [50]. Hence, ABCG2 was not considered specific to the limbal region according to our selection criteria. In the case of ΔNp63α, an isoform of p63, there were seven different probes on the array to identify p63, and the limbus had the highest expression levels detected by three of these probes but did not reach the twofold cut off level. Dr. Shigeru Kinoshita's group [51] showed that ΔNp63α was expressed in the basal and suprabasal layers in the epithelial cells in the limbus and conjunctiva, but at a slight lesser degree in the latter. The β isoform of the p63 appeared to be the most specific to the basal epithelium in the limbus. To further confirm their findings, QRT–PCR using isotype specific primers would be necessary.

On the basis of the EASE annotation, we found that melanin metabolism was among the leading biological processes in the limbus in vervet monkey. This result is
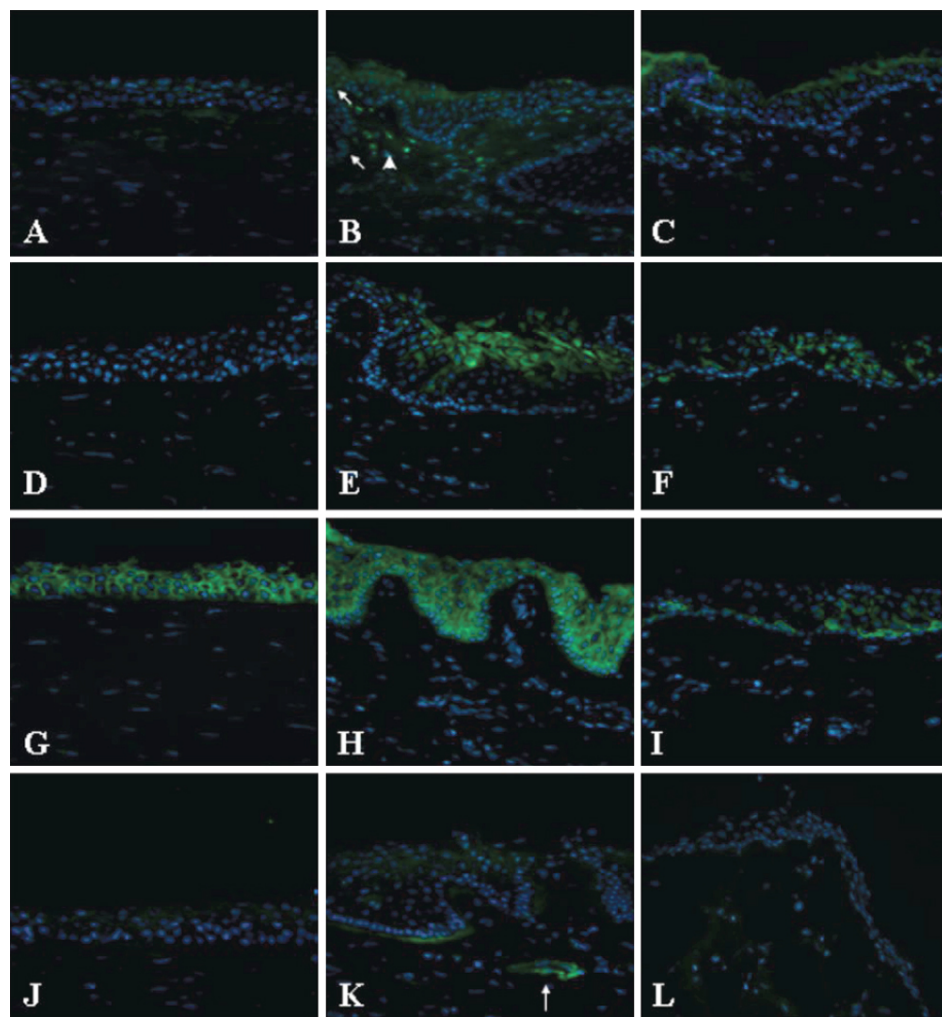
Figure 4. Protein expression of four selected genes in the cornea, limbus and conjunctiva by immunohistochemistry study. The left column was cornea (A,D,G,F). The middle was limbus (B,E,H,K), and the right was conjunctiva (C,F,I,L). HOP (green, A-C) was localized to the nucleus (blue) of a subgroup of basal limbal epithelial cells (B, arrows) and stromal cells (arrow head). K13 (green, D-F) was expressed in the suprabasal limbal (E) and conjunctival (F) epithelium and absent in the cornea (C). PERP (green, G-I) was localized to all layers of the epithelium in all three tissues. TNC (green, J-L) was localized specifically at the basement membrane of the limbus and blood vessel walls (arrow).

consistent with the observation that the limbus of the vervet monkey is highly pigmented. The palisades of Vogt, which is where LSCs are thought to reside, contain pigment granules that are aligned with the microplicae of the epithelium in human [6]. The melanocytes are scattered in the basal limbus epithelium [52]. Exposure to ultraviolet rays causes oxidative insult, DNA damage, and cell death in the corneal epithelia [53,54]. Epidermal melanocytes appear to play an important role in protecting epidermal tissue from oxidative damage. In addition, melanin pigmentation directly blocks ultraviolet radiation [55]. A recent article proposed that N-cadherin+ limbal melanocytes might be a cellular component of the LSC niche [8]. Whether melanocytes indeed constitute the LSC niche has yet to be confirmed. Nevertheless, there is mounting evidence that melanocytes play an important role in protecting neighboring cells from environmental insults.

Cell-cell adhesion was another highly noticeable biological process in the limbus. P-cadherin and TNC have been previously shown to be expressed preferentially in the extracellular matrix of the limbus in adults [17,20,56,57].

Cadherins play important roles in cell adhesion, motility, and development [58]. P-cadherin is most abundant in the placenta [59] and is restricted to the basal or lower layers of stratified epithelia including the prostate and skin and also to the breast myoepithelial cells [60,61]. Its aberrant expression is implicated to the cause of increased invasiveness of breast and cervical cancer [62]. TNC is another extracellular matrix protein that is only expressed at the basal membrane of the limbal epithelium (Figure 4). This finding is consistent with those of previous observations [56,57]. It is one of the nonstructural extracellular matrix proteins that are believed to regulate cell adhesion and migration and to have signal-altering functions [31,32]. More importantly, TNC is expressed in several stem niches including the nervous system [63,64], skin [65], and hematopoietic system [66,67]. In the neuronal system, TNC functions as a modulator of growth factor responsiveness in the developing neuronal stem cell niche. It also plays a director role in the retention of hematopoietic progenitor cells via interaction with stromal cells in the hematopoietic stem cell microenvironment. The
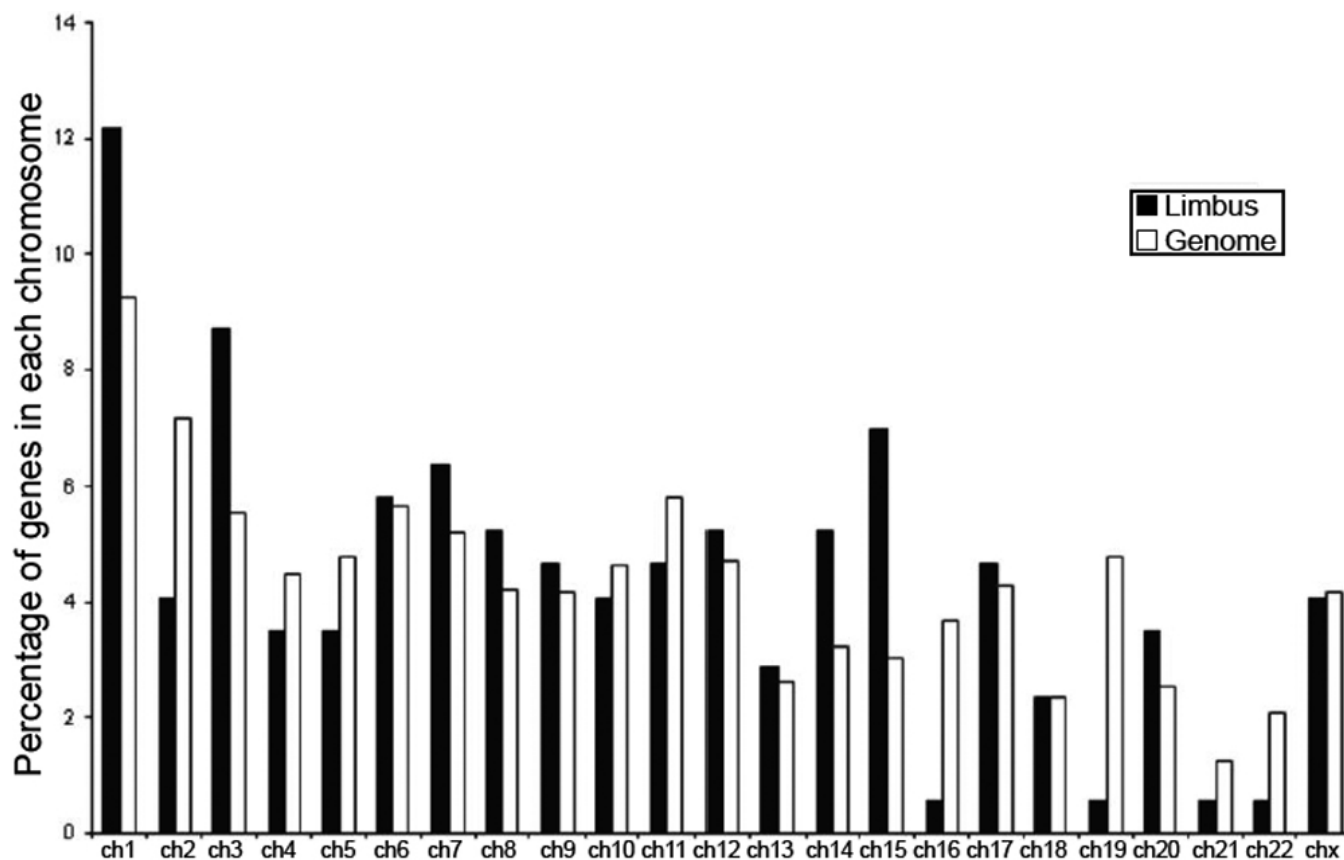
Figure 5. Chromosomal distribution of preferentially overexpressed genes in the limbus was disproportional to that of all other known human genes. Abbreviation: ch, chromosome.

specific distribution of both P-cadherin and TNC at the limbus is intriguing, and whether they play a similar role in the LSC niche is yet to be elucidated.

Our microarray data and immunohistochemistry studies showed that both K13 and HOP were preferentially expressed in the limbus, but their expression patterns were totally different. While K13 was predominantly expressed in the suprabasal epithelium, HOP was found in a subgroup of basal epithelial cells and stromal cells. Based on the expression pattern, K13 would not be a candidate of LSC marker. However, this finding indicates that the limbal suprabasal epithelia are different from those in the cornea or conjunctiva. HOP is an atypical homeobox gene that modulates cardiac development via cardiomyocyte differentiation and proliferation [27,68]. It interacts with serum response factor (SFR) and results in the inhibition of SRF-dependent cardiomyocyte specific genes. HOP is also expressed in the placenta and modulates the differentiation of trophoblastic cell lineage [69]. Our study is the first to identify that HOP is preferentially expressed in the basal limbal epithelial cells and the underlying stromal cells. Its unique anatomic expression suggests that it might also involve in the differentiation or proliferation of LSCs.

The chromosomal distribution of the limbus-specific genes was not random and was disproportionate to the general chromosome distribution of known human genes (Figure 5). Chromatin-remodeling factors are involved in maintaining chromatin structures and modulating gene expression in organisms ranging from yeast to human [70]. Previous studies showed that niche signals can regulate the renewing ability of stem cells at the chromatin level [71]. Whether the transcription of limbus-specific genes is regulated by chromosome-modeling factors as is the transcription of particular genes in embryonic stem cells and some adult stem cells is a very interesting idea, but its investigation is beyond the scope of the current study.

In summary, our microarray study has identified many genes that are preferentially expressed in the limbus of the vervet monkey that have not been reported previously. Expressions of HOP, TNC, K13 and PERP at the protein level are confirmed in humans. The findings of our study might provide valuable information in the molecular components and biological processes of limbal epithelial cells.

providing the vervet monkey eye tissues. This research was supported by the Emily G. Plumb Estate and Trust.

REFERENCES

1. Davanger M, Evensen A. Role of the pericorneal papillary structure in renewal of corneal epithelium. Nature 1971; 229:560-1. [PMID: 4925352]

2. Schermer A, Galvin S, Sun TT. Differentiation-related expression of a major 64K corneal keratin in vivo and in culture suggests limbal location of corneal epithelial stem cells. J Cell Biol 1986; 103:49-62. [PMID: 2424919]

3. Cotsarelis G, Cheng SZ, Dong G, Sun TT, Lavker RM. Existence of slow-cycling limbal epithelial basal cells that can be preferentially stimulated to proliferate: implications on epithelial stem cells. Cell 1989; 57:201-9. [PMID: 2702690]

4. Chen JJ, Tseng SC. Abnormal corneal epithelial wound healing in partial-thickness removal of limbal epithelium. Invest Ophthalmol Vis Sci 1991; 32:2219-33. [PMID: 1712763]

5. Dua HS, Joseph A, Shanmuganathan VA, Jones RE. Stem cell differentiation and the effects of deficiency. Eye 2003; 17:877-85. [PMID: 14631392]

6. Schlotzer-Schrehardt U, Kruse FE. Identification and characterization of limbal stem cells. Exp Eye Res 2005; 81:247-64. [PMID: 16051216]

7. Chen Z, de Paiva CS, Luo L, Kretzer FL, Pflugfelder SC, Li DQ. Characterization of putative stem cell phenotype in human limbal epithelia. Stem Cells 2004; 22:355-66. [PMID: 15153612]

8. Hayashi R, Yamato M, Sugiyama H, Sumide T, Yang J, Okano T, Tano Y, Nishida K. N-Cadherin is expressed by putative stem/progenitor cells and melanocytes in the human limbal epithelial stem cell niche. Stem Cells 2007; 25:289-96. [PMID: 17008425]

9. Li W, Hayashida Y, Chen YT, Tseng SC. Niche regulation of corneal epithelial stem cells at the limbus. Cell Res 2007; 17:26-36. [PMID: 17211449]

10. Schofield R. The relationship between the spleen colony-forming cell and the haemopoietic stem cell. Blood Cells 1978; 4:7-25. [PMID: 747780]

11. Kruse FE, Tseng SC. Growth factors modulate clonal growth and differentiation of cultured rabbit limbal and corneal epithelium. Invest Ophthalmol Vis Sci 1993; 34:1963-76. [PMID: 8491549]

12. Li L, Xie T. Stem cell niche: structure and function. Annu Rev Cell Dev Biol 2005; 21:605-31. [PMID: 16212509]

13. Espana EM, Kawakita T, Romano A, Di Pascuale M, Smiddy R, Liu CY, Tseng SC. Stromal niche controls the plasticity of limbal and corneal epithelial differentiation in a rabbit model of recombined tissue. Invest Ophthalmol Vis Sci 2003; 44:5130-5. [PMID: 14638708]

14. Goldberg MF, Bron AJ. Limbal palisades of Vogt. Trans Am Ophthalmol Soc 1982; 80:155-71. [PMID: 7182957]

15. Shortt AJ, Secker GA, Notara MD, Limb GA, Khaw PT, Tuft SJ, Daniels JT. Transplantation of ex vivo cultured limbal epithelial stem cells: a review of techniques and clinical results. Surv Ophthalmol 2007; 52:483-502. [PMID: 17719371]

16. Yen TH, Wright NA. The gastrointestinal tract stem cell niche. Stem Cell Rev 2006; 2:203-12. [PMID: 17625256]

17. Yeung AM, Schlotzer-Schrehardt U, Kulkarni B, Tint NL, Hopkinson A, Dua HS. Limbal epithelial crypt: a model for corneal epithelial maintenance and novel limbal regional variations. Arch Ophthalmol 2008; 126:665-9. [PMID: 18474777]

18. Dua HS, Shanmuganathan VA, Powell-Richards AO, Tighe PJ, Joseph A. Limbal epithelial crypts: a novel anatomical structure and a putative limbal stem cell niche. Br J Ophthalmol 2005; 89:529-32. [PMID: 15834076]

19. Adachi W, Ulanovsky H, Li Y, Norman B, Davis J, Piatigorsky J. Serial analysis of gene expression (SAGE) in the rat limbal and central corneal epithelium. Invest Ophthalmol Vis Sci 2006; 47:3801-10. [PMID: 16936091]

20. Figueira EC, Di Girolamo N, Coroneo MT, Wakefield D. The phenotype of limbal epithelial stem cells. Invest Ophthalmol Vis Sci 2007; 48:144-56. [PMID: 17197527]

21. Wolosin JM. Cell markers and the side population phenotype in ocular surface epithelial stem cell characterization and isolation. Ocul Surf 2006; 4:10-23. [PMID: 16669522]

22. Oshlack A, Chabot AE, Smyth GK, Gilad Y. Using DNA microarrays to study gene expression in closely related species. Bioinformatics 2007; 23:1235-42. [PMID: 17384014]

23. Nieto-Diaz M, Pita-Thomas W, Nieto-Sampedro M. Cross-species analysis of gene expression in non-model mammals: reproducibility of hybridization on high density oligonucleotide microarrays. BMC Genomics 2007; 8:89. [PMID: 17407579]

24. Gentleman RC, Carey VJ, Bates DM, Bolstad B, Dettling M, Dudoit S, Ellis B, Gautier L, Ge Y, Gentry J, Hornik K, Hothorn T, Huber W, Iacus S, Irizarry R, Leisch F, Li C, Maechler M, Rossini AJ, Sawitzki G, Smith C, Smyth G, Tierney L, Yang JY, Zhang J. Bioconductor: open software development for computational biology and bioinformatics. Genome Biol 2004; 5:R80. [PMID: 15461798]

25. Irizarry RA, Hobbs B, Collin F, Beazer-Barclay YD, Antonellis KJ, Scherf U, Speed TP. Exploration, normalization, and summaries of high density oligonucleotide array probe level data. Biostatistics 2003; 4:249-64. [PMID: 12925520]

26. Hosack DA, Dennis G Jr, Sherman BT, Lane HC, Lempicki RA. Identifying biologicaal themes within lists of genes with EASE. Genome Biol 2003; 4:R70. [PMID: 14519205]

27. Shin CH, Liu ZP, Passier R, Zhang CL, Wang DZ, Harris TM, Yamagishi H, Richardson JA, Childs G, Olson EN. Modulation of cardiac growth and development by HOP, an unusual homeodomain protein. Cell 2002; 110:725-35. [PMID: 12297046]

28. Corpuz LM, Funderburgh JL, Funderburgh ML, Bottomley GS, Prakash S, Conrad GW. Molecular cloning and tissue distribution of keratocan. Bovine corneal keratan sulfate proteoglycan 37A. J Biol Chem 1996; 271:9759-63. [PMID: 8621655]

29. Inatomi T, Spurr-Michaud S, Tisdale AS, Zhan Q, Feldman ST, Gipson IK. Expression of secretory mucin genes by human conjunctival epithelia. Invest Ophthalmol Vis Sci 1996; 37:1684-92. [PMID: 8675412]

30. Yoshida S, Shimmura S, Kawakita T, Miyashita H, Den S, Shimazaki J, Tsubota K. Cytokeratin 15 can be used to identify the limbal phenotype in normal and diseased ocular

surfaces. Invest Ophthalmol Vis Sci 2006; 47:4780-6. [PMID: 17065488]

31. Orend G, Chiquet-Ehrismann R. Adhesion modulation by antiadhesive molecules of the extracellular matrix. Exp Cell Res 2000; 261:104-10. [PMID: 11082280]

32. Hsia HC, Schwarzbauer JE. Meet the tenascins: multifunctional and mysterious. J Biol Chem 2005; 280:26641-4. [PMID: 15932878]

33. Kawakami Y, Eliyahu S, Delgado CH, Robbins PF, Rivoltini L, Topalian SL, Miki T, Rosenberg SA. Cloning of the gene coding for a shared human melanoma antigen recognized by autologous T cells infiltrating into tumor. Proc Natl Acad Sci USA 1994; 91:3515-9. [PMID: 8170938]

34. Tai T, Eisinger M, Ogata S, Lloyd KO. Glycoproteins as differentiation markers in human malignant melanoma and melanocytes. Cancer Res 1983; 43:2773-9. [PMID: 6850592]

35. Bennett DC. Colour genes, oncogenes and melanocyte differentiation. J Cell Sci 1991; 98:135-9. [PMID: 1905299]

36. Hearing VJ, Tsukamoto K. Enzymatic control of pigmentation in mammals. FASEB J 1991; 5:2902-9. [PMID: 1752358]

37. Kobayashi T, Vieira WD, Potterf B, Sakai C, Imokawa G, Hearing VJ. Modulation of melanogenic protein expression during the switch from eu- to pheomelanogenesis. J Cell Sci 1995; 108:2301-9. [PMID: 7673350]

38. Marks MS, Seabra MC. The melanosome: membrane dynamics in black and white. Nat Rev Mol Cell Biol 2001; 2:738-48. [PMID: 11584301]

39. Filenius S, Tervo T, Virtanen I. Production of fibronectin and tenascin isoforms and their role in the adhesion of human immortalized corneal epithelial cells. Invest Ophthalmol Vis Sci 2003; 44:3317-25. [PMID: 12882776]

40. Nose A, Nagafuchi A, Takeichi M. Isolation of placental cadherin cDNA: identification of a novel gene family of cell-cell adhesion molecules. EMBO J 1987; 6:3655-61. [PMID: 3428270]

41. Xu L, Overbeek PA, Reneker LW. Systematic analysis of E-, N- and P-cadherin expression in mouse eye development. Exp Eye Res 2002; 74:753-60. [PMID: 12126948]

42. Mbalaviele G, Nishimura R, Myoi A, Niewolna M, Reddy SV, Chen D, Feng J, Roodman D, Mundy GR, Yoneda T. Cadherin-6 mediates the heterotypic interactions between the hemopoietic osteoclast cell lineage and stromal cells in a murine model of osteoclast differentiation. J Cell Biol 1998; 141:1467-76. [PMID: 9628901]

43. Shimoyama Y, Takeda H, Yoshihara S, Kitajima M, Hirohashi S. Biochemical characterization and functional analysis of two type II classic cadherins, cadherin-6 and −14, and comparison with E-cadherin. J Biol Chem 1999; 274:11987-94. [PMID: 10207020]

44. Nishimura I, Muragaki Y, Hayashi M, Ninomiya Y, Olsen BR. Tissue-specific expression of type IX collagen. Ann N Y Acad Sci 1990; 580:112-9. [PMID: 2186688]

45. Gipson IK. The epithelial basement membrane zone of the limbus. Eye 1989; 3:132-40. [PMID: 2515978]

46. Tisdale AS, Spurr-Michaud SJ, Rodrigues M, Hackett J, Krachmer J, Gipson IK. Development of the anchoring structures of the epithelium in rabbit and human fetal corneas. Invest Ophthalmol Vis Sci 1988; 29:727-36. [PMID: 3366564]

47. Hopfer U, Fukai N, Hopfer H, Wolf G, Joyce N, Li E, Olsen BR. Targeted disruption of Col8a1 and Col8a2 genes in mice leads to anterior segment abnormalities in the eye. FASEB J 2005; 19:1232-44. [PMID: 16051690]

48. Kljuic A, Bazzi H, Sundberg JP, Martinez-Mir A, O'Shaughnessy R, Mahoney MG, Levy M, Montagutelli X, Ahmad W, Aita VM, Gordon D, Uitto J, Whiting D, Ott J, Fischer S, Gilliam TC, Jahoda CA, Morris RJ, Panteleyev AA, Nguyen VT, Christiano AM. Desmoglein 4 in hair follicle differentiation and epidermal adhesion: evidence from inherited hypotrichosis and acquired pemphigus vulgaris. Cell 2003; 113:249-60. [PMID: 12705872]

49. Barrans JD, Ip J, Lam CW, Hwang IL, Dzau VJ, Liew CC. Chromosomal distribution of the human cardiovascular transcriptome. Genomics 2003; 81:519-24. [PMID: 12706110]

50. Budak MT, Alpdogan OS, Zhou M, Lavker RM, Akinci MA, Wolosin JM. Ocular surface epithelia contain ABCG2-dependent side population cells exhibiting features associated with stem cells. J Cell Sci 2005; 118:1715-24. [PMID: 15811951]

51. Kawasaki S, Tanioka H, Yamasaki K, Connon CJ, Kinoshita S. Expression and tissue distribution of p63 isoforms in human ocular surface epithelia. Exp Eye Res 2006; 82:293-9. [PMID: 16115622]

52. Higa K, Shimmura S, Miyashita H, Shimazaki J, Tsubota K. Melanocytes in the corneal limbus interact with K19-positive basal epithelial cells. Exp Eye Res 2005; 81:218-23. [PMID: 16080916]

53. Rogers CS, Chan LM, Sims YS, Byrd KD, Hinton DL, Twining SS. The effects of sub-solar levels of UV-A and UV-B on rabbit corneal and lens epithelial cells. Exp Eye Res 2004; 78:1007-14. [PMID: 15051481]

54. Choy CK, Benzie IF, Cho P. UV-mediated DNA strand breaks in corneal epithelial cells assessed using the comet assay procedure. Photochem Photobiol 2005; 81:493-7. [PMID: 15773793]

55. Prota G. Pigment cell research: what directions? Pigment Cell Res 1997; 10:5-11. [PMID: 9170157]

56. Schlotzer-Schrehardt U, Dietrich T, Saito K, Sorokin L, Sasaki T, Paulsson M, Kruse FE. Characterization of extracellular matrix components in the limbal epithelial stem cell compartment. Exp Eye Res 2007; 85:845-60. [PMID: 17927980]

57. Maseruka H, Ridgway A, Tullo A, Bonshek R. Developmental changes in patterns of expression of tenascin-C variants in the human cornea. Invest Ophthalmol Vis Sci 2000; 41:4101-7. [PMID: 11095602]

58. Harrington MJ, Hong E, Fasanmi O, Brewster R. Cadherin-mediated adhesion regulates posterior body formation. BMC Dev Biol 2007; 7:130. [PMID: 18045497]

59. Shimoyama Y, Yoshida T, Terada M, Shimosato Y, Abe O, Hirohashi S. Molecular cloning of a human Ca2+-dependent cell-cell adhesion molecule homologous to mouse placental cadherin: its low expression in human placental tissues. J Cell Biol 1989; 109:1787-94. [PMID: 2793940]

60. Nose A, Takeichi M. A novel cadherin cell adhesion molecule: its expression patterns associated with implantation and organogenesis of mouse embryos. J Cell Biol 1986; 103:2649-58. [PMID: 3539943]

61. Daniel CW, Strickland P, Friedmann Y. Expression and functional role of E- and P-cadherins in mouse mammary ductal morphogenesis and growth. Dev Biol 1995; 169:511-9. [PMID: 7781895]

62. Paredes J, Albergaria A, Oliveira JT, Jeronimo C, Milanezi F, Schmitt FC. P-cadherin overexpression is an indicator of clinical outcome in invasive breast carcinomas and is associated with CDH3 promoter hypomethylation. Clin Cancer Res 2005; 11:5869-77. [PMID: 16115928]

63. von Holst A. Tenascin C in stem cell niches: redundant, permissive or instructive? Cells Tissues Organs 2008; 188:170-7. [PMID: 18160825]

64. Garcion E, Halilagic A, Faissner A. ffrench-Constant C. Generation of an environmental niche for neural stem cell development by the extracellular matrix molecule tenascin C. Development 2004; 131:3423-32. [PMID: 15226258]

65. Kloepper JE, Tiede S, Brinckmann J, Reinhardt DP, Meyer W, Faessler R, Paus R. Immunophenotyping of the human bulge region: the quest to define useful in situ markers for human epithelial hair follicle stem cells and their niche. Exp Dermatol 2008; 17:592-609. [PMID: 18558994]

66. Ohta M, Sakai T, Saga Y, Aizawa S, Saito M. Suppression of hematopoietic activity in tenascin-C-deficient mice. Blood 1998; 91:4074-83. [PMID: 9596652]

67. Klein G, Beck S, Muller CA. Tenascin is a cytoadhesive extracellular matrix component of the human hematopoietic microenvironment. J Cell Biol 1993; 123:1027-35. [PMID: 7693718]

68. Chen F, Kook H, Milewski R, Gitler AD, Lu MM, Li J, Nazarian R, Schnepp R, Jen K, Biben C, Runke G, Mackay JP, Novotny J, Schwartz RJ, Harvey RP, Mullins MC, Epstein JA. Hop is an unusual homeobox gene that modulates cardiac development. Cell 2002; 110:713-23. [PMID: 12297045]

69. Asanoma K, Kato H, Yamaguchi S, Shin CH, Liu ZP, Kato K, Inoue T, Miyanari Y, Yoshikawa K, Sonoda K, Fukushima K, Wake N. HOP/NECC1, a novel regulator of mouse trophoblast differentiation. J Biol Chem 2007; 282:24065-74. [PMID: 17576768]

70. Becker PB, Horz W. ATP-dependent nucleosome remodeling. Annu Rev Biochem 2002; 71:247-73. [PMID: 12045097]

71. Xi R, Xie T. Stem cell self-renewal controlled by chromatin remodeling factors. Science 2005; 310:1487-9. [PMID: 16322456]

The print version of this article was created on 5 November 2008. This reflects all typographical corrections and errata to the article through that date. Details of any changes may be found in the online version of the article.